Hopping conduction and persistent photoconductivity in Cu_2ZnSnS_4 thin films

J C González, G M Ribeiro, E R Viana, P A Fernandes, P M P Salomé, K Gutiérrez, A Abelenda, F M Matinaga, J P Leitão and A F da Cunha

Abstract

The temperature dependence of electrical conductivity and the photoconductivity of polycrystalline Cu_2ZnSnS_4 were investigated. It was found that at high temperatures the electrical conductivity was dominated by band conduction and nearest-neighbour hopping. However, at lower temperatures, both Mott variable-range hopping (VRH) and Efros–Shklovskii VRH were observed. The analysis of electrical transport showed high doping levels and a large compensation ratio, demonstrating large degree of disorder in Cu_2ZnSnS_4. Photoconductivity studies showed the presence of a persistent photoconductivity effect with decay time increasing with temperature, due to the presence of random local potential fluctuations in the Cu_2ZnSnS_4 thin film. These random local potential fluctuations cannot be attributed to grain boundaries but to the large disorder in Cu_2ZnSnS_4.

1. Introduction

Cu_2ZnSnS_4 (CZTS) polycrystalline thin films are potential candidates for a new generation of solar cell absorber layers due to their excellent physical properties such as a direct band gap close to 1.5 eV and a high absorption coefficient ($\alpha > 10^4\,cm^{-1}$) [1, 2]. In addition, natural abundance and relatively low cost of pure Cu, Zn and Sn make this material very interesting as a low-cost substitute of the absorber material $CuInGaSe_2$ (CIGS) in thin-film solar cells. The best conversion efficiency attained so far in a sulfur-based CZTS solar cells is around 8.4% [3]. Short minority carrier diffusion length and lifetime in the CZTS absorber layer, and a high series resistance of the devices attributed to a Schottky barrier due to the presence of a MoS_x layer at the interface between the CZTS absorber layer and the Mo back contact have been pointed out as factors that reduce the solar cell efficiency [4, 5]. Strong research efforts have been made in the study of different CZTS synthesis routes [3–10], CZTS structural and optical properties [2, 6–8], as well as in the development of CZTS solar cells [3–5, 9, 10]. However, very little is known about the electrical transport and photoconductivity properties of CZTS thin films and further studies are required.

The study of the temperature dependence of electrical transport in semiconductor materials is very important for the knowledge of material parameters, the understanding of the transport and microscopic mechanisms of charge transfer, as well as for the optimization and design of solar cells. Very recently, we have shown that the radiative and non-radiative recombination mechanisms in CZTS thin films are strongly

influenced by the doping level and degree of compensation, creating local potential fluctuations in those films [11]. The presence of acceptor centres, traps and local potential fluctuations can lead to the degradation of the performance of solar cells due to light-induced metastabilities associated with the persistent photoconductivity (PPC) effect [12, 13].

In this work, we present a study of the temperature dependence of the electrical conductivity of CZTS thin films by means of Hall effect and electrical conductivity measurements. In addition, photoconductivity measurements as a function of temperature are also presented. It will be shown that as the temperature decreases the electrical conductivity of the sample is dominated by band conduction, followed by nearest-neighbour hopping (NNH) and variable-range hopping (VRH). Both Mott-VRH and Efros–Shklovskii (ES) VRH were observed at low temperatures. An analysis of the electrical transport shows that the sample is heavily doped and compensated. Several important properties of the material, such as free carrier density and mobility above room temperature, acceptor and donor density, compensation ratio, grain potential barrier (GPB) height and density of traps at the grain boundaries, were extracted from the analysis of the electrical transport data. Photoconductivity studies showed the presence of the PPC effect, which lasts for more than 100 s and can be observed even at 320 K. The PPC decay time increases with temperature. This unexpected result is explained in terms of the presence of local potential fluctuations in the CZTS thin film due to the high doping levels and large compensation ratio.

2. Materials and methods

2.1. Sample preparation

The CZTS thin films were prepared by sequential deposition of precursor thin layers of Zn, Sn and Cu on a soda-lime glass (SLG) substrate followed by a sulfurization step. The precursor deposition was carried out by dc magnetron sputtering and sulfurization by thermal annealing in a sulfur vapour atmosphere [6, 7]. In order to make accurate transport measurements and to avoid any possible influence of the generally observed MoS_x layer at the Mo/CZTS interface [5], the CZTS thin film studied here was deposited directly on the SLG substrate. However, the morphology, chemical composition, crystalline structure, as well as optical properties of this sample are similar to those prepared using the Mo layer. The samples were also etched in a KCN solution in order to remove unwanted $Cu_{2-x}S$ phases. It can be expected that the CZTS thin films directly deposited on SLG substrates do not have exactly the same properties of those deposited on Mo-covered SLG substrates, due to the potential diffusion of sodium into the CZTS film [14]. Sodium diffusion into CZTS critically depends on the Mo layer deposition conditions and can be as high as in samples prepared without the Mo layer [14]. The addition of sodium significantly increases the grain size of the polycrystalline film [15, 16], the free carrier concentration [16] and the concentration of compensating donors [17]. However, the morphology, chemical composition, crystalline structure, as well as optical properties of our sample are similar to those prepared using the Mo layer. No sodium was observed in the sample by wavelength dispersive x-ray spectroscopy, the grain size did not increase with respect to the films deposited on Mo-covered SLG substrates and the concentration of compensating donors was found to be elevated. With the exception of the avoided Mo layer, this is a standard synthesis method used to grow the absorber layer of CZTS and CZTSe solar cells [5, 10, 18] and produces good-quality polycrystalline CZTS thin layers [2, 6, 7, 11].

2.2. Sample characterization

The morphology, crystalline structure and chemical composition of the samples were studied by scanning electron microscopy (SEM), x-Ray diffraction (XRD), Raman spectroscopy and inductively coupled mass spectrometry (ICP-MS).

The electrical transport properties were studied as a function of temperature by Hall effect measurements in the 305–370 K range, as well as by electrical conductivity $\sigma(T)$ measurements in the 16–400 K extended range. These measurements were carried out in darkness and in the van der Pauw configuration. Photoconductivity measurements were also carried out as a function of temperature, illuminating the sample with a 1.32 eV light-emitting diode (LED). The LED emission energy is lower than the band gap of CZTS (1.5 eV), therefore, band-to-band transitions were not excited in our experiments.

3. Results and discussion

Figure 1(*a*) shows the surface morphology of a CZTS thin film as obtained by SEM. The film is compact and polycrystalline with some voids on the surface, likely due to the removal of unwanted $Cu_{2-x}S$ phases during the KCN etching process. Figure 1(*b*) shows the XRD diffractogram of the CZTS thin film. Only peaks of the CZTS phase with a preferential (1 1 2) orientation are observed in the diffractogram. The crystallite size was estimated at 146 nm from the full-width at half-maximum peak and using the Scherrer formula [19]. The Raman spectrum of the film is also shown in figure 1(*c*). The Raman spectrum is dominated by CZTS peaks; however, residual amounts of ZnS were also detected [6].

ICP-MS measurements revealed atomic concentration ratios of [Cu]/([Zn] + [Sn]) = 0.9 and [Zn]/[Sn] = 1.3. The CZTS films were intentionally grown slightly off stoichiometry, to be close to the composition of the best CZTS solar cells [9, 20].

The temperature dependence of the electrical conductivity of a CZTS film is shown in figure 2. Hall effect measurement results are presented in the inset of figure 2. These measurements revealed p-type conductivity with a high concentration of free holes ($p_{\mathrm{Hall}} \sim 10^{18}\,\mathrm{cm}^{-3}$) and low mobility ($\mu_{\mathrm{Hall}} \sim 2.5\,\mathrm{cm}^2\,\mathrm{V}^{-1}\,\mathrm{s}^{-1}$). It was not possible to measure the Hall effect below 300 K. However, the analysis of the σ (T) data can give additional information about the electrical transport properties of the CZTS thin films.

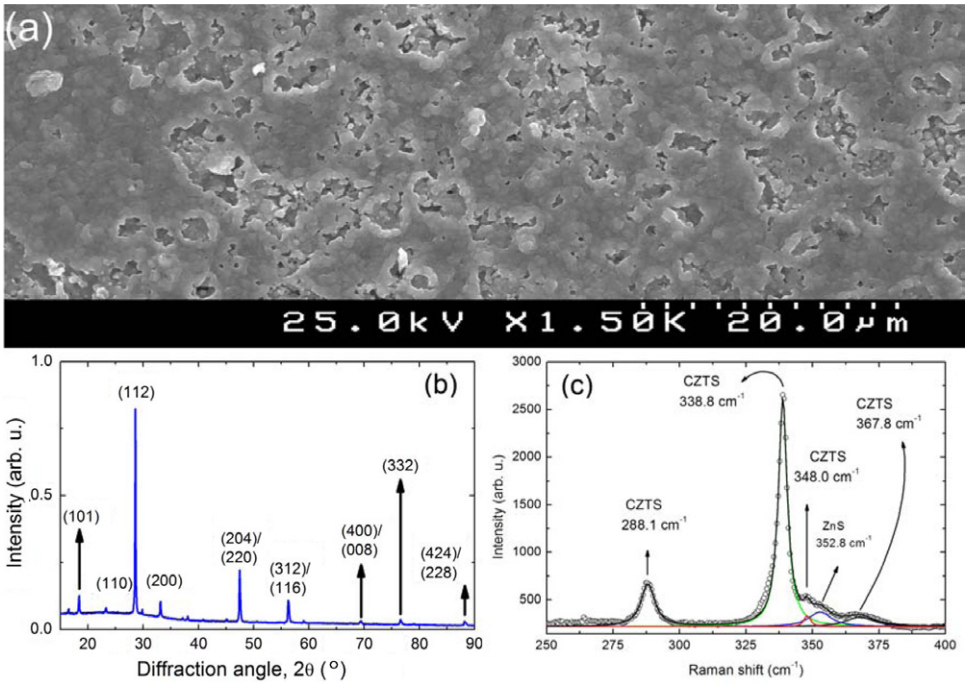

Figure 1. (*a*) Scanning electron micrograph of a CZTS thin film surface. (*b*) XRD diffractogram of the film. (*c*) Raman spectrum of the film.

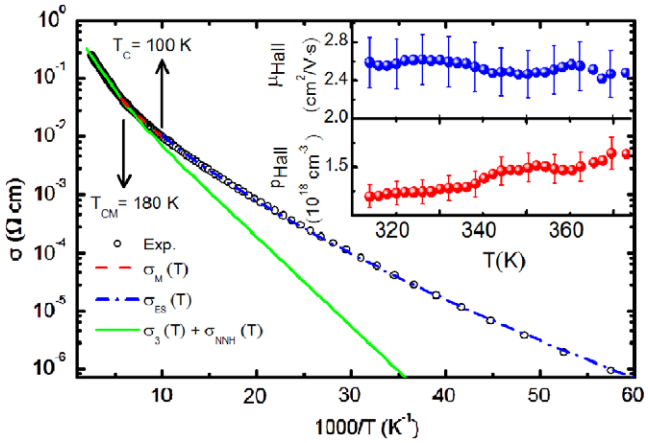

Figure 2. Temperature dependence of electrical conductivity. The solid line corresponds to the fitting of the data with $\sigma(T) = \sigma_3(T) + \sigma_{\mathrm{NNH}}(T)$ for $T > 180$ K, $\sigma_{\mathrm{M}}(T)$ for $100\,\mathrm{K} < T < 180\,\mathrm{K}$ and $\sigma_{\mathrm{ES}}(T)$ for $T < 100$ K. The inset shows the Hall mobility and concentration as a function of temperature.

Figure 2 shows that the σ (T) data can be divided into two different regions, at high and low temperatures. At high temperatures ($T > 180$ K), σ (T) is dominated by conduction in the bands and NNH conduction. At lower temperatures, the conductivity shows a typical VRH behaviour [21, 22].

At high temperatures, the electrical conductivity of the polycrystalline thin films is dominated by thermal emission of carriers over the inter-GPBs GPB [23]. The temperature dependence of the electrical conductivity of the p-type polycrystalline thin film can then be expressed as [23, 24]

$$\sigma_3(T) = ep\mu(T) = \sigma_0 T^{-1/2} \exp\left(-\frac{\phi}{k_{\mathrm{B}}T}\right), \tag{1}$$

where e is the electron charge, p is the free hole concentration, $\mu(T)$ is the free hole mobility due to grain boundaries, σ_0 is a constant, k_{B} is the Boltzmann constant, and the exponential factor describes the thermal activation of the carrier mobility flowing over the GPB with height ϕ. In polycrystalline thin films, the GPB height can be related to the doping level p, the dielectric permittivity ε and the trap density N_{t} at the grain boundary according to [25]

$$\phi = \frac{eN_{\mathrm{t}}^2}{8\varepsilon p}. \tag{2}$$

As temperature decreases, for p-type semiconductors, most of the free holes are recaptured by the acceptors. Then the holes do not have sufficient thermal energy to be excited from the acceptor levels to the valence band [26, 27]. In this case, the band conduction becomes less important, and hole hopping directly between acceptor states in the impurity band will be the main contributor to the conduction mechanism [26, 27]. If the compensation ratio is very high, the Fermi level will be located in the impurity band. Conduction of a compensated sample in this case is realized through NNH of charge carriers with small activation energy directly over impurity states. The conductivity in the NNH model is given by [28]

$$\sigma_{\mathrm{NNH}}(T) = \sigma_1 \exp\left(-\frac{E_{\mathrm{NNH}}}{k_{\mathrm{B}}T}\right), \tag{3}$$

$$E_{\mathrm{NNH}} = \frac{0.99e^2 N_{\mathrm{A}}^{1/3}}{4\pi\varepsilon}, \tag{4}$$

where σ_1 is a constant, N_{A} is the acceptor concentration, E_{NNH} is the activation energy for hole hopping and ε is the dielectric permittivity of CZTS [29].

Considering that both, band conduction and NNH conduction, mechanisms act in the high-temperature range of the data it is possible to extract some of the above-mentioned parameters by fitting of the conductivity data with $\sigma(T) = \sigma_3(T) + \sigma_{\mathrm{NNH}}(T)$. These conduction mechanisms explain well our data for $T > 180\,\mathrm{K}$. The result of the fitting is shown in figure 2, with $\sigma_0 = (27.8 \pm 0.3)\,\Omega^{-1}\,\mathrm{cm}^{-1}$, $\phi = (75.4 \pm 0.3)$ meV, $\sigma_1 = (0.23 \pm 0.01)\,\Omega^{-1}\,\mathrm{cm}^{-1}$ and $N_A = (3.1 \pm 0.2) \times 10^{18}\,\mathrm{cm}^{-3}$. In addition, from (2) the trap density at the grain boundaries $N_t = 1.7 \times 10^{12}\,\mathrm{cm}^{-2}$ can be obtained. This is of the same order of magnitude as the corresponding value for polycrystalline Si ($3 \times 10^{12}\,\mathrm{cm}^{-2}$) [25].

At lower temperatures, electron hopping between nearest neighbour sites is not always favoured due to the significant energy difference of the levels [21]. Then electrons prefer to jump to a more energetically similar and remote site. Therefore, in disordered or highly compensated materials the mechanism of electrical conduction changes from NNH to Mott-VRH at a critical temperature T_{CM}. VRH conduction was originally developed by Mott [21], pointing out that if there is a constant density of states (DOS) N_0 (E_F) near the Fermi level the conductivity is given by [21, 30]

$$\sigma_M(T) = \sigma_{0M} T^{-1/2} \exp\left[-\left(\frac{T_M}{T}\right)^{1/4}\right] \quad \text{and}$$

$$T_M = \frac{\alpha}{k_B \xi^3 N_0(E_F)}, \tag{5}$$

where σ_{0M} is a constant, T_M measures the degree of disorder in the film, $\alpha = 18.1$ is a constant, and ξ is the localization length which characterizes the hopping probability between sites.

This $T^{1/4}$ Mott's law has been observed in various classes of lightly doped semiconductors [21, 22, 30–32]. Nevertheless, a large body of literature reported $T^{1/2}$ at low temperatures instead of Mott's law [22, 31–34]. Efros and Shklovskii [22] argued that the Coulomb interaction would open a soft gap in the DOS, which leads to

$$\sigma_{ES}(T) = \frac{\sigma_{0ES}}{T} \exp\left[-\left(\frac{T_{ES}}{T}\right)^{1/2}\right] \quad \text{and}$$

$$T_{ES} = \frac{\beta e^2}{\varepsilon k_B \xi}, \tag{6}$$

where σ_{0ES} and $\beta = 2.8$ are constants.

As the temperature further decreases, the Coulomb effect becomes important and the conductivity crosses over from the Mott-VRH to the ES-VRH regime. Following Mott and ES theories, and ignoring here the slow temperature variation of the pre-exponential factors (σ_{0M} and σ_{0ES}) in (5) and (6), the crossover temperature can be determined by plotting $\ln(W)$ versus $\ln(T)$ [33, 34], where

$$W = \frac{\mathrm{d}[\ln(\sigma)]}{\mathrm{d}T} = p\frac{T_0^p}{T^{p+1}} \tag{7}$$

and T_0 corresponds to the characteristic temperature of the hopping mechanism ($T_0 = T_M$ for Mott-VRH, $T_0 = T_{ES}$ for ES-VRH) and p is the critical exponent of the hopping mechanism ($p = 0.25$ for Mott-VRH, $p = 0.5$ for ES-VRH).

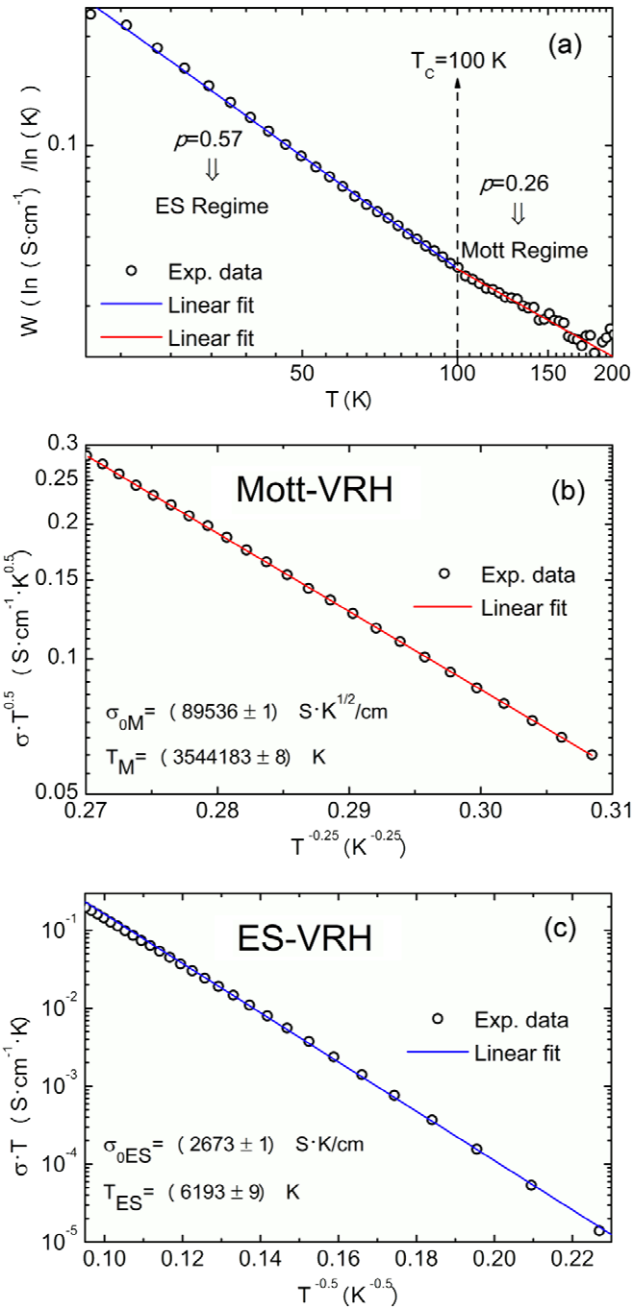

Figure 3. Temperature dependence of (*a*) W, (*b*) Mott-VRH, (*c*) ES-VRH. The solid lines correspond to the fitting of the data in (*a*), (*b*) and (*c*) with (7), (5) and (6), respectively.

Applying this method to our data, in figure 3(*a*), two different regimes with $p = 0.26$ (180–100 K) and $p = 0.57$ (100–16 K) can be observed. The first regime with $p = 0.26$ corresponds to the Mott-VRH conductivity, while the second regime with $p = 0.57$ corresponds to the ES-VRH conductivity. The Mott-VRH to ES-VRH crossover temperature T_c was found to be 100 K. Now, the hopping parameters can be obtained by fitting the $\sigma(T)$ data with (5) and (6), in their respective temperature interval, as shown in figures 3(*b*) and (*c*). The values of the hopping parameters are summarized in table 1.

In disordered or highly compensated materials there is a critical temperature T_{CM} for transition from the NNH to

Table 1. Values of the hopping parameters.

T_M (K)	T_{ES} ($\times 10^1$ K)	σ_{0M} (S K$^{1/2}$ cm^{-1})	σ_{0ES} (S K cm^{-1})
3544 183 ± 8	6193 ± 9	89 536 ± 1	2673 ± 1

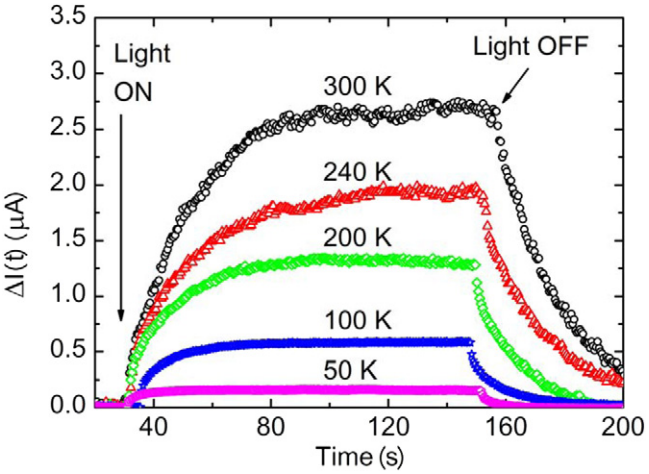

Figure 4. Time dependence of the induced photocurrent and persistent photocurrent for several temperatures.

the Mott-VRH. We have experimentally determined this value as 180 K. However, T_{CM} was also theoretically calculated by Shklovskii for compensation ratios k larger than 0.5 as [35]

$$T_{CM} = \frac{e^2 N_A^{2/3} \xi}{4\pi\varepsilon k_B}. \tag{8}$$

Furthermore, the compensation ratio, for $k > 0.5$, can be calculated from the knowledge of N_0 (E_F) by [35]

$$N_0(E_F) = \frac{2\varepsilon}{e^2} N_A^{2/3} (1-k)^{4/3}. \tag{9}$$

From (5), (8) and (9) the values of $\xi = 3.4$ nm, $N_0(E_f) = 1.5 \times 10^{18}$ cm^{-3} eV^{-1} and $k = 0.83$ were obtained.

The high values of T_M and T_{ES} reveal a large degree of disorder due to the large compensation ratio and doping levels [36]. Previous photoluminescence studies [11] revealed that a large compensation ratio and high doping levels lead to local potential fluctuations in CZTS thin films.

The signature of local potential fluctuations can also be observed in photoconductivity experiments by the presence of PPC after the excitation flux of photons is turned off. Figure 4 shows the time dependence of the photocurrent measurements for several temperatures, measured at a constant bias of 5 V and excitation power density of 0.742 W m^{-2}. When the excitation light from the LED is turned on the induced photocurrent increases rapidly, reaching a saturation value that increases with temperature. As soon as the excitation light is turned off the photocurrent slowly decreases, showing persistent behaviour. Figure 5 shows the decay PPC curves of the CZTS thin film as a function of temperature. The kinetics of these curves can be well described by a stretched exponential function:

$$\Delta I(t) = \Delta I_0 \exp\left[-\left(\frac{t}{\tau}\right)^{\beta}\right], \tag{10}$$

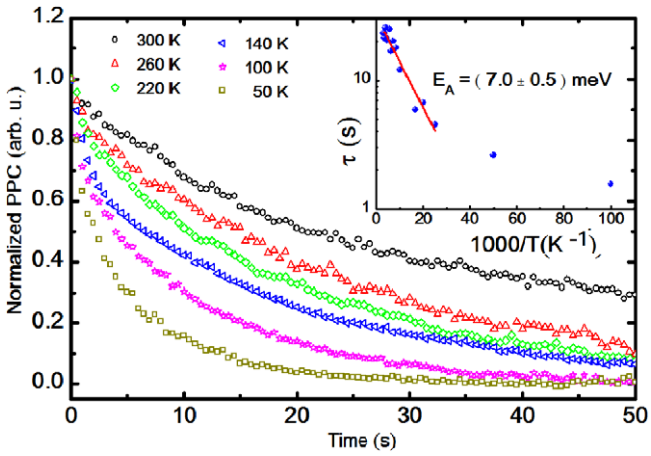

Figure 5. Persistent photoconductivity decay curves. The inset shows the temperature dependence of the decay time. The solid line corresponds to the fitting of an Ahrrenius function to the experimental data.

where $\Delta I(t) = I(t) - I_d$, $\Delta I_0 = I(0) - I_d$, τ is the decay time and β means the stretching exponent. I_d is the dark current, $I(t)$ is the measured current, and $I(0)$ is the saturated photocurrent value at the moment the excitation light is turned off.

Several models have been proposed to understand the origin of PPC in semiconductors. The PPC is believed to be either due to the presence of random local potential fluctuations causing the photogenerated electron–hole pair to spatially separate before the recombination occurs [37–39] or due to the presence of deep-lying traps such as DX [40, 41] and EL2 [42–44] centres, which capture the free carriers and re-emit slowly, resulting in an excess of conductivity even after the excitation light is cut off.

Let us now try to understand the results of figure 5 in the light of existing models. We observe a large PPC even after a few ten seconds of cutting off the light. The large PPC, even after 100 s of cutting off the light at room temperature, suggests the presence of random local potential fluctuations or deep-lying traps in the sample. Deep-lying traps are not expected to be responsible for the observed PPC in our case since then τ should decrease as the temperature increases [40–44]. On the other hand, in our case, we observed a large increase in τ with temperature. The temperature dependence of τ, as extracted from the fitting of (10) to the experimental data, is shown in the inset of figure 5. Therefore, the PPC in the CZTS thin film should be related to random local potential fluctuations. This anomalous behaviour of τ with temperature has also been observed in CdS nanorods [37] and ZnCdSe crystals [38, 39] and explained in terms of random local potential fluctuations. The random local potential fluctuations could be at the grain boundaries or in the CZTS grains due to the large compensation ratio and doping levels. When the light is turned on, photogenerated carriers are generated uniformly in the films. Some of these carriers recombine rapidly, whereas others are separated due to random local potential fluctuations [37–39]. Thus, the electrons and holes accumulate at spatially different regions in the corresponding local potential minima and a large PPC with slow decay is observed. The temperature

dependence of τ shows Arrhenius behaviour with an activation energy of 7 meV. This activation energy E_A corresponds to the energy barrier that the carries have to overcome in order to recombine. The exact mechanism relating the random local fluctuations to the PPC is under further experimental and theoretical investigation. However, hopping conductivity, PPC effect and similar decay time behaviour with temperature were observed in several studied CZTS samples. Furthermore, since the GPB height ($\phi = 75.4$ meV) is ten times larger than the PPC energy barrier ($E_b = 7$ meV) the random local potential fluctuations should be related not to the GPB, but to disorder due to high doping levels and large compensation ratio that creates potential fluctuations in the bulk of the grains. This interpretation is in agreement with the observed hopping conduction and the photoluminescence results already reported for CZTS [11] thin films.

4. Conclusions

The temperature dependence of the electrical conductivity of polycrystalline CZTS thin films was investigated. The analysis of Hall effect and electrical conductivity measurements showed that the CZTS thin films are p-type and highly doped. It was found that at temperatures higher than 180 K the electrical conductivity of the sample is dominated by band conduction and NNH. However, at lower temperatures both Mott-VRH and ES-VRH were observed. A Mott- to ES-VRH regime crossover was determined at approximately 100 K. The analysis of electrical transport showed a high compensation ratio $k = 0.83$, a GPB height $\phi = (75.4 \pm 0.3)$ meV, acceptor density $N_A = (3.1 \pm 0.2) \times 10^{18}$ cm^{-3}, and trap density at the grain boundaries $N_t = 1.7 \times 10^{12}$ cm^{-2}. Photoconductivity studies showed the presence of the PPC effect in the sample. The PPC decay time was found to anomalously increase with temperature. This result was explained in terms of the presence of random local potential fluctuations in the CZTS thin film. These random local potential fluctuations were attributed not to the grain boundaries but to the large disorder in the CZTS thin film, in agreement with the hopping conduction observed in the electrical conductivity experiments.

Acknowledgments

We gratefully acknowledge the financial support from the Portuguese Science and Technology Foundation (FCT) through the grants PEst-C/CTM/LA0025/2011, PTDC/CTMMET/113486/2009, REDE/1509/RME/2005, 411.00 and 3779-08-4, as well as the Brazilian agencies CAPES, CNPq and FAPEMIG.

References

[1] Jae-Seung S, San-Yul L, Jae-Choon L, Hyo-Duk N and Kyoo-Ho K 2003 *Sol. Energy Mater. Sol. Cells* **75** 155
[2] Leitão J P, Santos N M, Fernandes P A, Salomé P M P, da Cunha A F, González J C and Matinaga F M 2011 *Thin Solid Films* **519** 7390
[3] Shin B, Gunawan O, Zhu Y, Bojarczuk N A, Chey S J and Guha S 2011 *Prog. Photovolt: Res. Appl.* **21** 72–6
[4] Shin B, Wang K, Gunawan O, Reuter K B, Chey S J, Bojarczuk N A, Todorov T, Mitzi D B and Guha S 2011 High efficiency $Cu_2ZnSn(S_xSe_{1-x})_4$ thin film solar cells by thermal co-evaporation, *37th IEEE Photovoltaic Specialists Conf. (PVSC) (Seattle, WA, 19–24 June 2011)* pp 002510–002514
[5] Fernandes P A, Sartori A F, Salomé P M P, Malaquias J, da Cunha A F, Graça M P F and González J C 2012 *Appl. Phys. Lett.* **100** 233504
[6] Fernandes P A, Salomé P M P and da Cunha A F 2009 *Thin Solid Films* **517** 2519
[7] Fernandes P A, Salomé P M P and da Cunha A F 2009 *Semicond. Sci. Technol.* **24** 105013
[8] Fernandes P A, Salomé P M P and da Cunha A F 2010 *J. Phys. D: Appl. Phys.* **43** 215403
[9] Katagiri H 2005 *Thin Solid Films* **480** 426
[10] Fernandes P A, Salomé P M P, da Cunha A F and Schubert B A 2011 *Thin Solid Films* **519** 7382
[11] Leitão J P, Santos N M, Fernandes P A, Salome P M P, da Cunha A F, González J C, Ribeiro G M and Matinaga F M 2011 *Phys. Rev.* B **84** 024120
[12] Rau U, Schmitt M, Parisi J, Riedl W and Karg F 1998 *Appl. Phys. Lett.* **73** 223
[13] Meyer T, Schmidt M, Engelhardt F, Parisi J and Rau U 1999 *Eur. Phys. J.: Appl. Phys.* **8** 43
[14] Yoon J H, Cho S, Kim W M, Park J K, Baik Y J, Lee T S, Seong T Y and Jeong J H 2011 *Sol. Energy Mater. Sol. Cells* **95** 2959
[15] Hlaing W M, Johnson J L, Bhatia A, Lund E A, Nowell M N and Scarpulla M A 2011 *J. Electron. Mater.* **40** 2214
[16] Prabhakar T and Jampana N 2011 *Sol. Energy Mater. Sol. Cells* **95** 1001
[17] Schroeder D J and Rockett A A 1997 *J. Appl. Phys.* **82** 4982
[18] Salomé P M P, Fernandes P A, da Cunha A F, Leitão J P, Malaquias J, Weber A, González J C and da Silva M I N 2010 *Sol. Energy Mater. Sol. Cells* **94** 2176
[19] Kril C E and Birringer R 1998 *Phil. Mag.* A **77** 621–40
[20] Todorov T K, Reuter K B and Mitzi D B 2010 *Adv. Mater.* **22** E156
[21] Mott N F and Davis E A 1971 *Electronic Processes in Noncrystalline Materials* (Belfast, Oxford: Clarendon)
[22] Efros A L and Shklovskii B I 1985 *Electronic Properties of Doped Semiconductors* (Berlin: Springer)
[23] Bube R H 1975 *Annu. Rev. Mater. Sci.* **5** 201
[24] Look D C 1989 *Electrical Characterization of GaAs Materials and Devices* (New York: Wiley)
[25] Seto J Y W 1975 *J. Appl. Phys.* **46** 5247
[26] Ma J, Wang Y, Ji F, Yu X and Ma H 2005 *Mater. Lett.* **59** 2142
[27] Miller A and Abrahams E 1960 *Phys. Rev.* **120** 745
[28] Shklovskii B I 1972 *Fiz. Tekh. Poluprov.* **6** 1197
Shklovskii B I 1973 *Sov. Phys.—Semicond.* **6** 1053 (Engl. Transl.)
[29] Person C 2010 *J. Appl. Phys.* **107** 053710
[30] Paul D K and Mitra S S 1973 *Phys. Rev. Lett.* **31** 1000
[31] Viana E R, González J C, Ribeiro G M and Oliveira A G 2012 *Phys. Status Solidi RRL* **6** 262
[32] Kosyak V, Karmarkar M A and Scarpulla M A 2012 *Appl. Phys. Lett.* **100** 263903
[33] Hill R M 1976 *Phys. Status Solidi* a **35** K29
[34] Zabodskii A G 1998 *Phys.—Usp.* **41** 722
[35] Tauc J C and Menth A 1972 *J. Non-Cryst. Solids* **8** 569
[36] Pollak M and Ortuño M 1985 *Electron–Electron Interactions in Disordered Systems* (Amsterdam: North-Holland)
[37] Paul G S and Agarwal P 2009 *J. Appl. Phys.* **106** 103705
[38] Lin J Y and Jiang H X 1990 *Phys. Rev.* B **41** 5178

[39] Dissanayake A S, Huang S X, Jiang H X and Lin J Y 1990 *Phys. Rev.* B **44** 13343
[40] Chadi D J and Chang K J 1988 *Phys. Rev. Lett.* **61** 873
[41] Lin J Y, Dissanayake A, Brown G and Jiang H X 1990 *Phys. Rev.* B **42** 5855
[42] Rubinger R M, Bezerra J C, Chagas E F, Gonzalez J C, Rodrigues W N, Ribeiro G M, Moreira M V B and de Oliveira A G 1999 *J. Appl. Phys.* **84** 3764
[43] Parker J C and Bray R 1988 *Phys. Rev.* B **38** 3610
[44] Nojima S 1985 *J. Appl. Phys.* **57** 620